Available online at www.sciencedirect.com

ScienceDirect

Procedia CIRP 60 (2017) 26 – 31

www.elsevier.com/locate/procedia

27th CIRP Design 2017

Adaptive Measurement and Modelling Methodology for In-line 3D Surface Metrology Scanners

Manoj Babu* , Pasquale Franciosa, Darek Ceglarek

WMG, University of Warwick, Coventry, UK

* Corresponding author. Tel.: +44(0)24 7657 4501; *E-mail address:* M.K.Babu@warwick.ac.uk

Abstract

3D surface metrology scanners are primarily used for surface reconstruction in reverse engineering and for off-line inspection of parts but, their application potential for in-line process control remains largely unexplored. The lack of usage of 3D surface metrology scanners for in-line process control can be attributed to the large processing time of metrology equipment compared to the cycle time of automotive assembly systems. To overcome this challenge, a novel methodology for adaptive measurement and modelling of data captured by in-line 3D surface measurement systems is proposed in this paper. The methodology models part deviations by augmenting the scanner data with spatio-temporal correlations in deviation field and enables efficient implementation of in-line part shape measurement for process control. The proposed methodology consists of two steps: (i) modelling deviations to enable prediction of entire part deviations with partial measurements, and; (ii) adaptively selecting part regions to be measured by taking into account the measurement data available from the scanner up to current time-step. The partial measurement strategy based on deviation modeling and adaptive region selection results in maximum information gain within the given assembly system cycle time. The prediction of entire part surface deviation with higher confidence leads to effective identification of part-to-part defect variation patterns. The proposed methodology is demonstrated on an automotive door component.

Peer-review under responsibility of the scientific committee of the 27th CIRP Design Conference

Keywords: In-line process control; 3D surface scanner; In-line adaptive measurement; Spatio-temporal deviation modelling.

1. Introduction

Efforts to make manufacturing smart have led to increased automation and the use of a multitude of sensors for monitoring manufacturing and assembly process. Of the many tasks the sensors accomplish, quality control is an important one and is carried out though different types of metrological devices. Various quality control methodologies for manufacturing systems exist [1], but are aimed at point-based measurements which are mainly off-line with a few in-line solutions. However, in-line metrology systems lead to higher productivity and reduced costs compared to off-line methods and sometimes is the only solution to enforce strict tolerances [2]. The use of in-line metrology devices in conjunction with closed-loop systems for proactive control of the assembly process rather than passive monitoring greatly increases the efficiency of manufacturing process.

Frameworks for implementing in-line closed-loop process control from the perspective of cyber-physical systems have been proposed in [3] and [4], however many aspects of implementational hurdles are yet to be addressed. Though closed-loop systems have been used to control quality of printed circuit assemblies [5], injection molding process [6]; a sheet-metal assembly system with in-line 3D surface measurement exhibiting several unique challenges is considered in the present study.

Existing literature for metrology in assembly process mainly focus on methods for inspection of parts and propose various sampling methodologies. These sampling methodologies can be classified as applicable to two kinds of systems: (1) point-based measurement systems, and; (2) 3D surface measurement or Cloud of Points (CoP) based systems. For point-based measurements systems, adaptive sapling has been proposed in [7]–[12]. Kriging [13] based methodologies have been

Peer-review under responsibility of the scientific committee of the 27th CIRP Design Conference
doi:10.1016/j.procir.2017.01.009

employed in all these studies to ascertain tolerance requirements during inspection and optimise the sequence of sampling for Co-ordinate Measuring Machine (CMM), which are mostly off-line. In-line point-based measurements with optical coordinate measurement machines have been used in industry for 100% dimensional inspections [14], however they are static and measure a fixed set of points on each part. For 3D surface measurement a dynamic off-line inspection method was developed in [15] to obtain high quality CoPs of parts using feedback from previous measurements to optimise next view point of the sensor considering shadows and surface reflection. A Statistical Process Control (SPC) methodology for CoP data from a laser scanner was proposed in [16]. The methodology applies Q-Q plots to identify quality defects, however the method requires entire part scans which cannot be obtained in-line. A summary of the afore-discussed literature is presented in Table 1. In this study, we address the challenges a 3D surface measurement system must overcome to enable in-line closed-loop quality control for an assembly system.

Two main challenges for in-line implementation of 3D surface based scanner for closed-loop quality control compared to point-based measurements are: (1) long processing time of the scanner; and (2) analysis of high dimensional data output from the scanner within the given cycle time of the assembly system. Since, the cycle time of the assembly system is 90-120 seconds and the time taken to measure the complete part, for instance a door panel is 4-10 minutes, complete measurement is infeasible. Thus, a partial measurement scheme and a methodology to identify the critical regions of a part to measure is essential.

The contribution of this paper is to address the aforementioned challenges by developing: (1) methodology to predict the entire deviation field of the part with partial measurement, utilizing spatio-temporal correlation in deviation field, and; (2) adaptive measurement strategy based on predicted deviations to identify the critical regions to be measured. Aforementioned contributions lead to effective in-line implementation of 3D surface scanner with higher confidence in predicted deviation field and with fewer measurements enabling better root cause identification. The remainder of the paper is organized as follows; Section 2 describes spatio-temporal correlation of a part in an assembly line as well as presents model development and lists the underlined assumptions. Section 3 describes the proposed methodology in detail, followed by Section 4, where the methodology is illustrated by an automotive door component as a case study. Finally, conclusion and future research directions are discussed in Section 5.

Table 1: Summary of literature for inspection and process control

	Point-based Measurements		3D Surface/ CoP-based Measurements	
	Off-line	**In-line**	**Off-line**	**In-line**
Fixed	Standard practice	Ceglarek et al. [14]	Wells et al. [16]	Proposed
Adaptive	Ascione et al. [8] Dumas et al. [9] Pedone et al. [12]	--	Shi et al.[15]	Proposed

2. Model development and assumptions

2.1. Spatio-temporal correlation in part deviation field

The concept of spatio-temporal correlation has traditionally been used in various applications such as disease mapping, weather prediction [17], [18] etc. We extend this concept to variation in the assembly process by considering a series of parts moving through the assembly line as shown conceptually in Fig. 1, from time (sample number) $t = 1$ to $t = 5$ and with part deviations from the design nominal marked by the intensity of color. Time t is used here to represent the sequence of parts in the assembly line. There exists a correlation in time between same locations on successive parts separated by time δt as the parts undergo the same series of processes in the assembly line giving rise to similar variations in time. This correlation in time is assumed to be continuous in the present study, i.e., the current part is directly related to the previous part/sub-assembly. In addition, points close to each other in a given part also have similar deviations (i.e. points are correlated spatially within the same part), which can be attributed to geometric covariance [19]. This is important in assembly process with compliant parts.

We utilize both the spatial and temporal correlation to model and predict variation in the assembly process. This correlation is incorporated in the prediction process through the covariance function of Gaussian Process (GP) which considers time as input dimension along with the location as detailed in the following paragraphs.

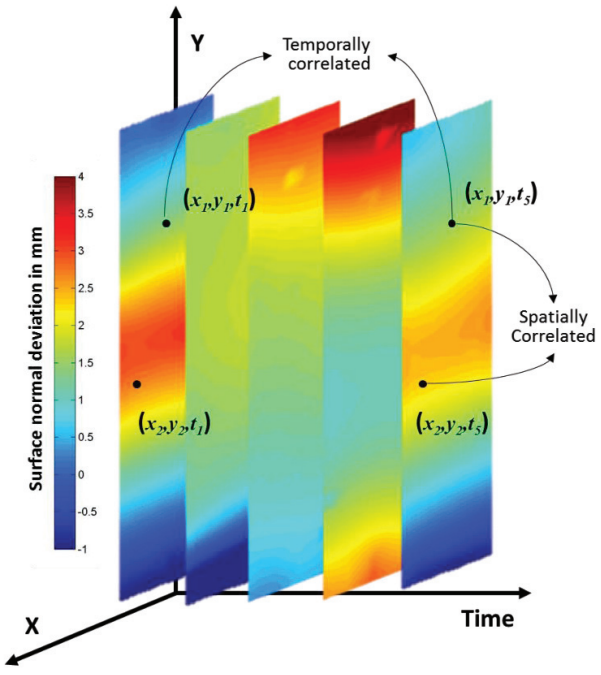

Figure 1: Representation of spatio-temporal correlation

2.2. Model development

List of variables

N =Number of nodes in the mesh representation of the part
x_i =Position of each node in Cartesian co-ordinates, $\forall i = 1,2...N$
y_i =The deviation of each node in surface normal direction, $\forall i = 1,2...N$
t =1, 2…T, the time variable representing the sequence of parts in the assembly line
$\tilde{x}_{it}$ =The augmented input variable $[x_i, t]$, S.T $\tilde{x}_{it} \in \mathbb{R}^4$, abbreviated as $\tilde{x}$
y_{it} =The deviation of i^{th} node, in surface normal direction at time t, abbreviated as y
Q =The number of nodes at which measurement is available

List of Parameters

l_i = Length of correlation along i^{th} dimension
σ_f = Scale parameter of the covariance function
σ_n = Noise parameter of the gaussian process

Notations

$\sim \mathcal{N}(\mu, \sigma^2)$ =A Gaussian distribution variable with mean μ and variance σ^2
$\sim \mathcal{GP}(m, k)$ =A Gaussian Process with mean function m and covariance function k
$\mathbb{E}[x]$ =Expected value of the random variable x

Firstly, CAD model of the part is converted to its mesh representation with N nodes, where the positon of each node is represented by x_i . The CoP obtained from the scanner is aligned and superimposed on the ideal mesh geometry from which, distance (y_i) in surface normal direction between the mesh node (x_i) and the CoP is calculated. We form augmented vector $\tilde{x}_{it} = [x_i, t]$ and $\tilde{y}_{it}$ the corresponding node deviation. The task now is to find a functional relationship $f : \tilde{x}_{it} \in \mathbb{R}^4 \rightarrow y_{it} \in \mathbb{R}$, which is modelled using Gaussian Process Regression (GPR) as

$$y_{it} = f(\tilde{x}_{it}) + \varepsilon \tag{1}$$

Where, ε is the Gaussian noise $\sim \mathcal{N}(0, \sigma_n^2)$, Eq. (1) implies that the deviation at a location y_{it} is a sum of a latent function $f(\tilde{x}_{it})$ and Gaussian noise ε . We perform Bayesian regression by assuming a Gaussian Process (GP) prior over $f(\tilde{x}_{it})$. A GP is defined as a collection of random variables, any finite number of which has a joint Gaussian distribution [20] and is completely specified by its mean function and covariance function. In the following discussion we represent $\tilde{x}_{it}$ as $\tilde{x}$, y_{it} as y and $\tilde{x}_{i't'}$ as $\tilde{x}'$ for notational simplicity and use the complete notation when necessary.

Defining the mean function $(m(\tilde{x}))$ and the covariance function $(k(\tilde{x}, \tilde{x}'))$ as, $\mathbb{E}[f(\tilde{x})]$ and $\mathbb{E}[(f(\tilde{x}) - m(\tilde{x}))(f(\tilde{x}') - m(\tilde{x}'))]$, we have the Gaussian process $f(\tilde{x}) \sim \mathcal{GP}(m(\tilde{x}), k(\tilde{x}, \tilde{x}'))$. While there are different types of mean and covariance functions, we will here use the zero mean function and the Squared Exponential (SE) covariance function given by Eq. (2)

$$k(\tilde{x}, \tilde{x}') = {\sigma_f}^2 \, \mathrm{e}^{\left(-\frac{1}{2}(\tilde{x}-\tilde{x}')L^{-1}(\tilde{x}-\tilde{x}')^{\mathrm{T}}\right)} \tag{2}$$

Where $L = diag\left(\left[l_i\right]_{i=1}^{4}\right)^{-2}$ with i = 1…4 representing the dimension of input space and ${\sigma^2}_f$ the scaling factor. Thus, the Gaussian process becomes $\sim \mathcal{GP}(0,\ k(\tilde{x}, \tilde{x}'))$. From Eq. (2) it can be seen that the covariance between outputs is expressed as a function of input locations, and, $\tilde{x}$ representing a point in $\mathbb{R}^4$, with time as a dimension takes care of temporal correlations along with spatial correlations. In GPR there is no formal distinction between space and time domain and the physical distinction has to be addressed through the covariance function [21]. The elements of the diagonal matrix L are called the length parameters or correlation lengths, which determine the distance up to which the correlation persists along a given direction.

When the deviation data $Y = [y_q]_{q=1}^{Q}$ at locations $X = [\tilde{x}_q]_{q=1}^{Q}$ is known, where, Q is the number of nodes at which deviation is identified through measurement. The prediction of magnitude of deviation y_* , at unknown location $\tilde{x}_*$ following [20] can be shown to be $\sim \mathcal{N}(\mathrm{f}_*, \mathbb{V})$, i.e. $p(y_* \mid \mathrm{X}, \mathrm{Y}, \tilde{x}_*)$ is Gaussian with mean f_* and variance $\mathbb{V}$ given by,

$$\begin{aligned} \mathrm{f}_* &= \mathbf{k}_* \left(K + {\sigma_n}^2 I\right)^{-1} Y \\ \mathbb{V} &= k(\tilde{x}_*, \tilde{x}_*) - \mathbf{k}_* \left(\mathbf{K} + {\sigma_n}^2 \mathbf{I}\right)^{-1} \mathbf{k}_*^{\mathrm{T}} \end{aligned} \tag{3}$$

Where, $\mathbf{k}_*$ is the vector obtained by evaluating $k(\tilde{x}_*, \tilde{x}_q)$ $\forall q = 1...Q$ and $\mathbf{K}$ the $Q \times Q$ matrix obtained by evaluating $k(\tilde{x}_q, \tilde{x}_{q'})$ $\forall q, q' = 1...Q$. The computations in the gaussian process regression scale $O(Q^3)$ in time, and can handle up to 10000 points within reasonable computation time. Equations (3) are equivalent to the prediction equations in Kriging with the similarities being explained in [20] and is the method applied in existing literature described in Section 1. However, when dealing with CoP data and large parts, Q, is almost always greater than 30000 points in a single time step and by considering temporal correlations the number further increases. In addition to this, the task of prediction of unknown deviation has to be performed in-line and real-time. A task that cannot be performed by simple GPR or Kriging described earlier and requires the use of approximation techniques that enable handling of large datasets in real-time.

For this task we implement the Sparse Online Gaussian Processes (SOGP) [22] taking into account the spatial and

temporal correlations in the deviation data, SOGP is an online version of Gaussian Processes (GP) capable of handling large datasets in real-time. The deviation predictions from SOGP as in the regular GP are probabilistic, providing error bounds or uncertainty in predicted deviations. This uncertainty along with the magnitude of predicted deviations are used to identify the critical regions to be measured as described in the following Section.

3. Methodology

The proposed methodology for in-line implementation of 3D surface scanner in an assembly system has two main highly interdependent components: (1) iterative deviation modelling and initial model development, and; (2) adaptive part measurement, schematically described in Fig. 2.

3.1. Iterative deviation modelling and initial model development

Since the large processing time of the 3D surface, scanner inhibits complete part measurement within the cycle time of the assembly system. We adaptively choose the regions to be measured and the model continuously assimilates data from these measurements, predicting the deviation at unmeasured regions. The continuous data assimilation is based on the principle of Bayesian online learning which updates the predictive distribution $p\left(y_* \mid \mathrm{X}, \mathrm{Y}, x_{Q+1}, y_{Q+1}\right)$, where Q+1 is the new measurement to be assimilated, iteratively rather than processing in a batch. This Bayesian update was parameterized in [22], giving the equations for mean and covariance for prediction at the location $\tilde{x}_*$ using Q+1 measurements as

$$\mathrm{f}\left(\tilde{x}_*\right)_{Q+1} = \boldsymbol{\alpha}_{Q+1}^{\mathrm{T}} \mathbf{k}\left(\tilde{x}_*\right)_{Q+1} \tag{4}$$

$$\mathbb{V}_{post}\left(\tilde{x}_*, \tilde{x}'\right)_{Q+1} = k\left(\tilde{x}_*, \tilde{x}'\right) + \mathbf{k}\left(\tilde{x}_*\right)_{Q+1}^{\mathrm{T}} \mathbf{C}_{Q+1} \mathbf{k}\left(\tilde{x}_*\right)_{Q+1} \tag{5}$$

Where, $\mathbf{k}\left(\tilde{x}_*\right)_{Q+1} = \left[k\left(\tilde{x}_*, \tilde{x}_q\right) \ \forall q = 1 \ldots (Q+1)\right]$, $\boldsymbol{\alpha}_{Q+1} = \boldsymbol{\alpha}_Q + w_1^{Q+1} \mathbf{s}_{Q+1}$, $\mathbf{s}_{Q+1} = \left(\mathbf{C}_Q \mathbf{k}_{Q+1} + e_{Q+1}\right)$, $\mathbf{C}_{Q+1} = \mathbf{C}_Q + w_2^{Q+1} \mathbf{s}_{Q+1} \mathbf{s}_{Q+1}^{\mathrm{T}}$, $\mathrm{e}_{Q+1} = [0, 0, \ldots 1]$, is the $(Q+1)^{\text{th}}$ unit vector, $w_2^{Q+1} = -1/\sigma_{Q+1}^2$, $w_1^{Q+1} = \left(y_{Q+1} - \mu_{Q+1}\right)/\sigma_{Q+1}^2$, $\mu_{Q+1}, \sigma_{Q+1}^2$ are predicted mean and variance at location $\tilde{x}_{Q+1}$ utilizing Q measurements.

It can be seen from Eqs. (4) and (5) that the size of $\boldsymbol{\alpha}$ and $\mathbf{C}$ increase continuously with Q and hence prediction of mean and variance become computationally expensive. To prevent this increase, the number of measurements Q to be stored and utilised for predicting deviation at unmeasured regions in limited to a set of basis vectors. The criteria for selection of these Basis Vectors (BV) is defined in [22], the size of BV are fixed based on computational capacity and size of part being measured.

Once new measurements are available from the scanner the learning process is restarted and BV vectors are updated and predictions are made for deviations in unmeasured regions with the confidence of prediction given by the estimate of variance

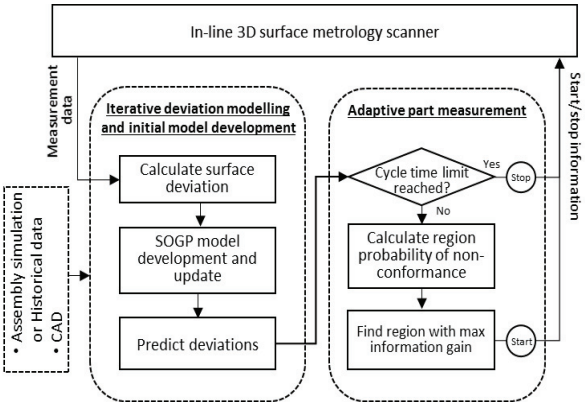

Figure 2: Overview of the proposed methodology

as in Eq. (5). The predictions made consider both spatial and temporal correlations as incorporated in the covariance function given by Eq. (2).

The parameters of the gaussian process regression as described in Section 2 are the mean function and covariance function parameters. Since, we assume the mean function to be zero, the parameters to be optimized are $\theta = \left[\sigma_f, \sigma_n, \left[l_i\right]_{i=1}^{4}\right]$. The optimization of these parameters is carried out by minimizing the negative log marginal likelihood, a robust option that prevents overfitting of the prediction model parameters to known measurement data. There are two options to generate the required data to optimise the parameters; 1) Assembly simulation and, 2) Learn the parameters completely online iteratively.

When deviation data from assembly simulation is used the parameters for the initial deviation prediction model are optimized by minimizing the negative log marginal likelihood through gradient descent. However, in scenarios where no data is available we optimise the parameters iteratively using the measurement data from the scanner by minimizing the leave-one-out negative log-likelihood with stochastic gradient descent averaged over every 10 measured deviations available, as described in [23].

3.2. Adaptive part measurement

The critical aspect of the methodology is to identify the regions of the parts to be measured which maximize the ability to predict the real deviation field of the parts as closely as possible. As described in Section 3.1 the predictions for deviations in unmeasured regions of the part are iteratively updated to incorporate the latest measurements. Once the latest predictions for mean and variance of deviations at unknown regions are available through Eqs. (4) and (5) we calculate a new metric P_{it}, the probability of non-conformance Eq. (6), which gives the total probability of a point being out of specification. Where, *normCDF* represents the cumulative normal density function, USL and LSL are Lower and Upper Specification Limits respectively. Probabilities P_1 and P_2 are calculated based on the predicted deviation at a given point which according to the GPR follows a gaussian distribution

with mean f_{it} and variance $\mathbb{V}_{it}$ and is schematically represented in Fig. 3.

$$P_{it} = P_1 + P_2 = \left(1 - normCDF\left((\mathrm{USL} - f_{it})/\sqrt{\mathbb{V}_{it}}\right)\right) + normCDF\left((\mathrm{LSL} - f_{it})/\sqrt{\mathbb{V}_{it}}\right) \quad (6)$$

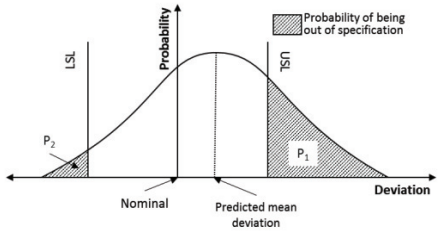

Figure 3: Representation of predicted probability of being out of specification

The probability of non-conformity is calculated for each point in a region and the expected information gain (or Entropy), I_r achieved by measuring a particular region is obtained by Eq. (7) [24]. Where, N_r is the total number of points in region r. The unmeasured region with maximum information gain is chosen to as the candidate for next measurement.

$$I_r = -\sum_{i=1}^{i=N_r} P_{it} \log(P_{it}) \quad (7)$$

3.3. Measurement stopping criteria

The measurement of the part can be stopped based on a combination of the following aspects: (1) The time available for measurements due to limitations in cycle time; (2) Reaching a given level of confidence in deviation pattern prediction, and; (3) Identification of root cause of the fault. In the present study we apply the cycle time criteria implicitly by limiting the number of regions of a part that can be measured.

4. Case study

4.1. Pre-processing and initial model development

The proposed methodology was implemented on an automotive door component (halo). The part is converted to a mesh representation consisting of trigular and tetrahedral elements with 37,000 nodes as shown in Fig. 4(b). The part being too large to be measured in one instance is segmented into smaller regions that approximately correspond to the field of view of the 3D surface scanner as shown in Fig. 4(c), the part under consideration was segmented into 25 regions. The parameters of the prediction model were trained based on two previous complete measures as shown in Fig. 4(a). The stochastic gradient descent yielded the optimum values for θ as [2.50, 0.046, 100.37, 97.39, 83.11, 118.50].

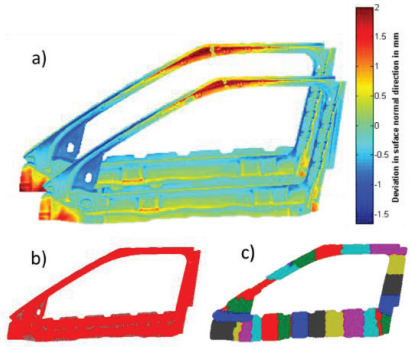

Figure 4: (a) Part with deviation from nominal used for training (b) Mesh representation of part (c) Part segmented into regions

4.2. In-line adaptive deviation modelling

In-line measurement is simulated by iteratively using the deviation data of one region at a time and adaptively identifying the next region to be measured. The criteria for adaptive selection is based on criteria explained in Section 3.2. The

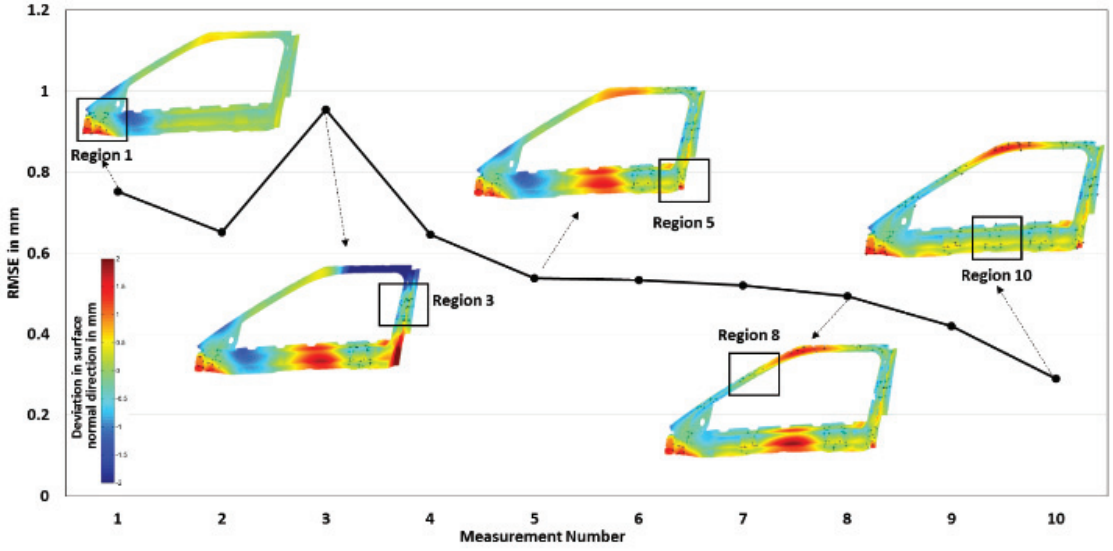

Figure 5: Adaptive measurement applied to automotive door component

results of iterative modelling and measurement are shown in Fig. 5 where, the predicted deviation after each measurement and the corresponding Root Mean Square Error (RMSE) is shown. It can be seen from Fig. 5 that the error monotonically reduces after the first three measurements. The present time required to process measurement of each region and make predictions for all unmeasured regions is around 3s and makes in-line application possible. The prediction after 10 measurements almost resembles the true part variations with a root mean square error of 0.29 mm compared to the complete measurement obtained after measuring 25 regions into which the part was segmented to. The aim of the present study is to identify the deviation patterns as closely as possible to the real deviation. It can also be seen that the regions with high deviations are correctly identified as illustrated in Fig. 6. Thus, reducing the number of measurements required and aiding in deviation pattern identification with higher confidence.

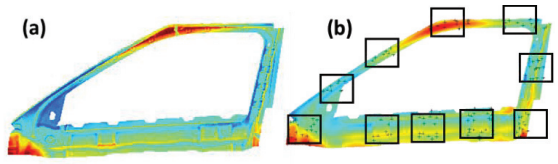

Figure 6: (a) True complete measurement (b) Predicted deviation with measured regions indicated

5. Conclusion

We proposed a novel methodology for in-line implementation of 3D surface scanner with adaptive measurements. The methodology incorporated spatio-temporal correlations through sparse online gaussian processes by which the measurements from the scanner were iteratively incorporated into the prediction model and the next region to be measured was adaptively found in real-time, on a criteria based on information gain. The developed methodology enables the implementation of an in-line closed-loop quality control system and identification of part deviation patterns with partial measurements. However the proposed model can further be improved by, (i) The incorporation non separable space-time covariance functions, which can capture the temporal dynamics of the system [25], (ii) Creating a library of most probable patterns through assembly simulation which can further reduce the total number of measurements required, and (iii) Relaxing the continuous time assumption which considers direct correlation with previous part, which might not necessarily be the case as successive parts sometimes are not be directly related. Aforementioned topics will be addressed in future research making the methodology robust.

Acknowledgements

This study has been supported by the UK EPSRC project EP/K019368/1: "Self-Resilient Reconfigurable Assembly Systems with In-process Quality Improvement."

References

[1] J. Shi and S. Zhou, "Quality control and improvement for multistage systems: A survey," *IIE Trans.*, vol. 41, no. 9, pp. 744–753, 2009.

[2] E. Savio, L. De Chiffre, S. Carmignato, and J. Meinertz, "Economic benefits of metrology in manufacturing," *CIRP Ann. - Manuf. Technol.*, vol. 65, no. 1, pp. 495–498, 2016.

[3] L. Monostori, B. Kádár, T. Bauernhansl, S. Kondoh, S. Kumara, G. Reinhart, O. Sauer, G. Schuh, W. Sihn, and K. Ueda, "Cyber-physical systems in manufacturing," *CIRP Ann. - Manuf. Technol.*, vol. 65, pp. 621–641, 2016.

[4] L. Wang, M. Törngren, and M. Onori, "Current status and advancement of cyber-physical systems in manufacturing," *J. Manuf. Syst.*, vol. 37, pp. 517–527, 2015.

[5] K. Feldmann and J. Sturm, "Closed Loop Quality Control in Printed Circuit Assembly," *IEEE Trans. Components Packag. Manuf. Technol. Part A*, vol. 17, no. 2, pp. 270–276, 1994.

[6] S. L. B. Woll and D. J. Cooper, "Pattern-based closed-loop quality control for the injection molding process," *Polym. Eng. Sci.*, vol. 37, no. 5, pp. 801–812, May 1997.

[7] P. Pedone, D. Romano, and G. Vicario, "New Sampling Procedures in Coordinate Metrology Based on Kriging-Based Adaptive Designs," *Stat. Innov. SE - 6*, pp. 103–121, 2009.

[8] R. Ascione, G. Moroni, S. Petrò, and D. Romano, "Adaptive inspection in coordinate metrology based on kriging models," *Precis. Eng.*, vol. 37, no. 1, pp. 44–60, 2013.

[9] A. Dumas, B. Echard, N. Gayton, O. Rochat, J. Y. Dantan, and S. Van Der Veen, "AK-ILS: An active learning method based on Kriging for the inspection of large surfaces," *Precis. Eng.*, vol. 37, no. 1, pp. 1–9, 2013.

[10] G. Moroni and S. Petrò, "Optimal inspection strategy planning for geometric tolerance verification," *Precis. Eng.*, vol. 38, no. 1, pp. 71–81, 2014.

[11] G. Barbato, E. M. Barini, P. Pedone, D. Romano, and G. Vicario, "Sampling Point Sequential Determination by Kriging for Tolerance Verification With CMM," in *Volume 1: Advanced Energy Systems; Advanced and Digital Manufacturing; Advanced Materials; Aerospace*, 2008, pp. 391–401.

[12] P. Pedone, G. Vicario, and D. Romano, "Kriging-based sequential inspection plans for coordinate measuring machines," *Appl. Stoch. Model. Bus. Ind.*, vol. 25, no. 2, pp. 133–149, Mar. 2009.

[13] J.-P. Chiles and Wiley InterScience (Online service), *Geostatistics modeling spatial uncertainty*. Wiley-Blackwell, 2011.

[14] D. Ceglarek and J. Shi, "Dimensional variation reduction for automotive body assembly," *Manuf. Rev.*, vol. 8, no. 2, pp. 139–154, 1995.

[15] Q. Shi, N. Xi, W. Sheng, and Y. Chen, "Development of dynamic inspection methods for dimensional measurement of automotive body parts," *Proc. - IEEE Int. Conf. Robot. Autom.*, vol. 2006, no. May, pp. 315–320, 2006.

[16] L. J. Wells, F. M. Megahed, C. B. Niziolek, J. a. Camelio, and W. H. Woodall, "Statistical process monitoring approach for high-density point clouds," *J. Intell. Manuf.*, vol. 24, no. 6, pp. 1267–1279, Jun. 2012.

[17] A. Brix and P. J. Diggle, "Spatiotemporal prediction for log-Gaussian Cox processes," *J. R. Stat. Soc. Ser. B (Statistical Methodol.*, vol. 63, no. 4, pp. 823–841, Nov. 2001.

[18] N. A. C. Cressie and C. K. Wikle, *Statistics for spatio-temporal data*. Wiley, 2011.

[19] K. G. Merkley, "Tolerance analysis of compliant assemblies," Brigham Young University, 1998.

[20] C. E. Rasmussen and C. K. I. Williams, *Gaussian processes for machine learning*. MIT Press, 2006.

[21] T. Gneiting and M. Schlather, "Space-Time Covariance ModelsBased in part on the article 'Space-time covariance models' by Tilmann Gneiting and Martin Schlather, which appeared in the *Encyclopedia of Environmetrics* .," *Encycl. Environmetrics*, pp. 10–13, 2013.

[22] L. Csato, "Gaussian Processes - Iterative Sparse Approximations," ASTON UNIVERSITY, 2002.

[23] H. Soh and Y. Demiris, "Spatio-Temporal Learning With the Online Finite and Infinite Echo-State Gaussian Processes," *IEEE Trans. Neural Networks Learn. Syst.*, vol. 26, no. 3, pp. 522–536, Mar. 2015.

[24] D. MacKay, *Information theory, inference and learning algorithms*. 2003.

[25] T. Gneiting, "Nonseparable, Stationary Covariance Functions for Space–Time Data," *J. Am. Stat. Assoc.*, vol. 97, no. 458, pp. 590–600, 2002.